Ionization of biological molecules by multicharged ions by using the stoichiometric model

(Dated: September 22, 2019)

Abstract

Contents

I. INTRODUCTION

The damage caused by the impact of multicharged heavy projectiles on biological targets has become a field of interest due to its recent implementation in ion–beam cancer therapy. The effectiveness of the radiation depends on the choice of the ions. In particular, theoretical and experimental studies with different projectiles have concluded that charged carbon ions could be the most suitable ions to be used. Nonetheless, the study of such systems represents a challenge from the theoretical point of view.

The ionization of biological molecules by multicharged ions constitutes the primary damage mechanism. The most widely used method to predict such processes is the first Born approximation. At high energies, this perturbative method warrants the Z^2 laws, where Z is the projectile charge. However, the damage is concentrated in the vicinities of the Bragg peak –at energies of hundreds of keV/amu–, precisely where the Born approximation starts to fail. Another theoretical issue arises due to the targets themselves; we are dealing with complex molecules, and the description of such targets represents a hard task for *ab initio*

calculations. The objective of this article is to deal with these two aspects; first, we perform more appropriate calculations on the primary damage mechanism, which can replace the Born results. Second, we inspect and test a stoichiometric model to describe the ionization of molecular targets.

To overcome the first perturbative approximation limitations, and since the projectiles are multicharged ions, we resort to the Continuum Distorted Wave–Eikonal Initial State (CDW), which includes higher perturbative corrections. We start from the premise that the ionization process is the mechanism that deposits the most significant amount of primary energy. Moreover, it is well known that the residual electrons from the ionization become a source of significant local biological damage. The secondary electrons are included in Monte Carlo simulations, and hence their behavior must be investigated. In Section II A and II B, we calculate the mean energy and angular distributions of the ejected electrons. Surprisingly, we found a substantial dependence of the charged projectile, which is unexpected in the first Born approximation. We deal with the molecular structure complexity of the target by implementing the simplest stoichiometric model (SSM): the molecules are assumed to be composed of isolated independent atoms, and the total cross–section by a linear combination of weighted atomic calculations.

By implementing the CDW and the SSM, we calculate ionization cross–section of several molecules of interest (see Table I) by the impact of antiprotons, H^+, He^{+2}, Be^{+4}, C^{+6}, and O^{+8}. In Section 3, we show our results for different DNA and RNA molecules, such as adenine, cytosine, guanine, thymine, uracil, tetrahydrofuran (THF), pyrimidine, and also DNA backbone. In Section III B, we test the Toburen scaling rule [25, 26], which states that the ratio between the ionization cross–section and the number of weakly bound electrons can be arranged in a narrow universal band in terms of the projectile velocity. We applied this rule to several hydrocarbons and nucleobases and noted that the width of the resulting universal band could be significantly reduced if we redefine the effective number of active electrons in the collision. The new scaling is then tested by comparison with experimental data.

Although the multicharged projectiles are dealt with the CDW, the stoichiometric model used seems to be very simplistic. The approach considers each atom as neutral, which is not correct. In Section 3.5, we used the molecular electronic structure code GAMESS [1] to calculate the excess or defect of electron density on the atoms composing the molecules.

Then, the SSM is modified to account for the departure from the neutrality of the atoms. We find that the modified SSM for the DNA molecules does not introduce substantial changes in the cross sections.

II. THEORY: IONIZATION OF ATOMS

In the present study, we consider six atoms, α = H, C, N, O, P, and S, and six projectiles, antiprotons $\bar{p}$, H^+, He^{+2}, Be^{+4}, C^{+6}, and O^{+8}. Most of the organic molecules are composed of these atoms. Some particular molecules also include halogen atoms such as fluor and bromine; ionization cross sections of these elements have been previously published [2, 3].

The total ionization cross sections of these atoms were calculated using the CDW [xxx]. The initial bound and final continuum radial wave functions were obtained by using the RADIALF code, developed by Salvat and co–workers [4], and a Hartree-Fock potential obtained from the Depurated Inversion Method [5, 6]. We used a few thousand pivot points to solve the Schrödinger equation, depending on the number of oscillations of the continuum state. The radial integration was performed using the cubic spline technique. The number of angular momenta considered varied from 8, at very low ejected-electron energies, up to 30, for the highest energies considered. The same number of azimuth angles were required to obtain the four-fold differential cross section. The calculation performed does not display prior-post discrepancies at all. Each atomic total cross section was calculated using 35 to 100 momentum transfer values, 28 fixed electron angles, and around 45 electron energies depending on the projectile impact energy. In our theoretical treatment, we expand our final continuum wave function as usual,

$$\psi^-_{\vec{k}}(\vec{r}) = \sum_{l=0}^{l_{\max}} \sum_{m=-l}^{l} R^-_{kl}(r) Y_l^m(\widehat{r}) Y_l^{m^*}(\widehat{k}) \,. \tag{1}$$

We are confident with our calculations up to $l_{\max} \sim 30$. Further details of the calculation are given in Ref. [7]. Simultaneously, we will be reporting state to state ionization cross sections for the 36 ion–target systems considered in the present work [8]. We expect that these results will be useful to estimate molecule fragmentation.

We report our total CDW ionization cross sections for the six essential elements by the impact of six projectiles in Fig. 1. To reduce the resulting 36 magnitudes into a single consistent figure, we considered the fact that in the first Born approximation the ionization

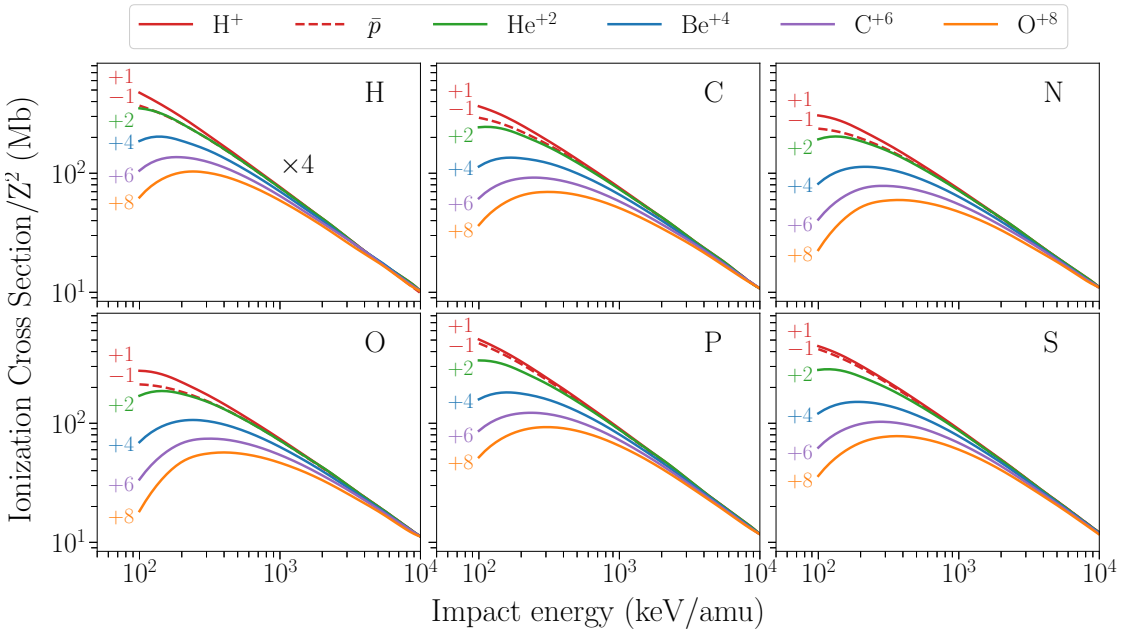

FIG. 1: Reduced CDW total ionization cross section of six atomic targets. The curves are labeled with the charge state corresponding to the six multicharged projectiles.

cross section scales with the square of the projectile charge, Z^2. The values of the impact energies considered range between 0.1 to 10 MeV/amu, where the CDW is supposed to hold. In fact, for the highest projectile charges the minimum impact energy where the CDW is expected to be valid could be higher than 100 keV. We also performed similar calculations with the first Born approximation, and we corroborated that it provides quite reliable results only for energies higher than a couple of MeV/amu. We use the same line color to indicate the projectile charge throughout all the figures of this work: dashed–red, solid–red, blue, magenta, olive and orange for antiprotons, H^+, He^{+2}, Be^{+4}, C^{+6}, and O^{+8}, respectively. Notably, there is no complete tabulation of ionization of atoms by the impact of multicharged ions. We hope that the ones presented in this article will be of help for future works.

A. Emitted electron energies

In a given biological medium, direct ionization by ion impact accounts for just a fraction of the overall damage. Secondary electrons, as well as recoil target ions, also contribute substantially to the total damage. We can consider the single differential cross section of

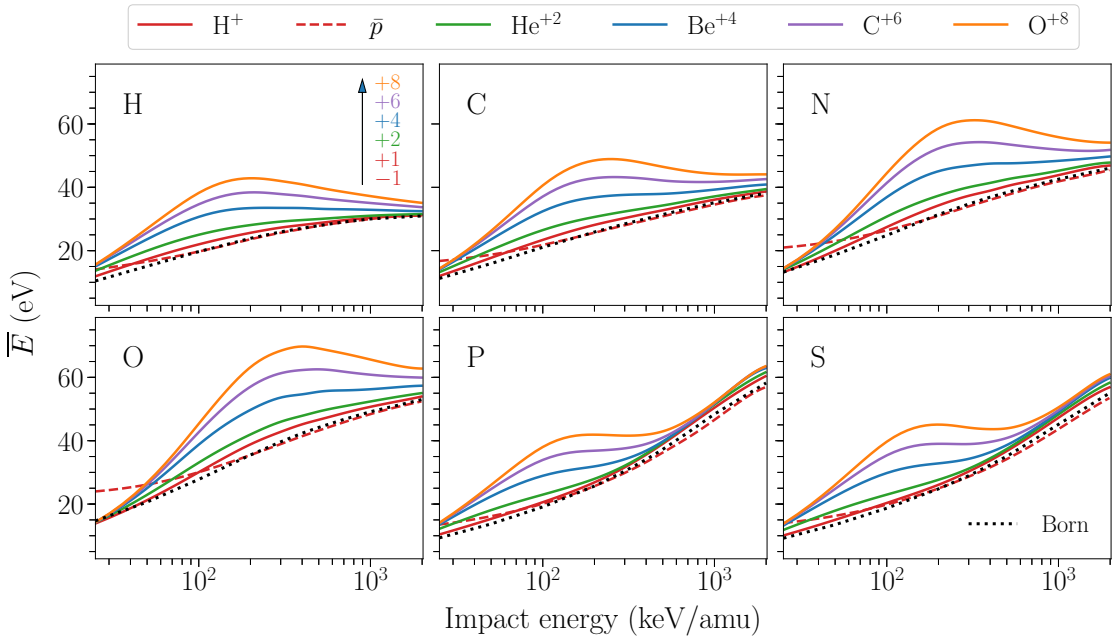

FIG. 2: Mean emitted energy distribution for ionization by impact of multicharged ions, given by Eq. (2). Dashed lines for $\bar{p}$, solid lines for ion charges +1, +2, +4, +6 and +8, as indicated.

the shell nl of the atom α, $d\sigma_{\alpha nl}/dE$, to be a function of the ejected electron energy E as a simple distribution function [27]. Then, we can define the mean value $\overline{E}_\alpha$ as in Ref. [28],

$$\overline{E}_\alpha = \frac{\langle E_\alpha \rangle}{\langle 1 \rangle} = \frac{1}{\sigma_\alpha} \sum_{nl} \int dE\, E \frac{d\sigma_{\alpha,nl}}{dE}\,, \tag{2}$$

$$\langle 1 \rangle = \sigma_\alpha = \sum_{nl} \int dE\, \frac{d\sigma_{\alpha,nl}}{dE}\,, \tag{3}$$

where Σ_{nl} takes into account the sum of the different sub–shell contributions of the element α.

The mean emitted electron energies $\overline{E}_\alpha$ for H, C, N, O, P and S are shown in Fig. 2. The range of impact velocities was shortened to $v = 10$ a.u. due to numerical limitations in the spherical harmonics expansion of Eq. (1). As the impact velocity v increases, so do $\langle E_\alpha \rangle$ and $l_{\max}$, which results in the inclusion of very oscillatory functions in the integrand. Furthermore, the integrand of $\langle E_\alpha \rangle$ includes the kinetic energy E (see Eq. (2)), which cancels the small energy region and reinforces the large values, making the result more sensible to large angular momenta. Regardless, for $v > 10$ a.u., the first Born approximation holds.

In Fig. 2, we estimate $\overline{E}_\alpha$ of the emitted electron in the 0.5–2.7 a.u. energy range, or equivalently from 15 to 70 eV, for all the targets. Our results agree with the experimental

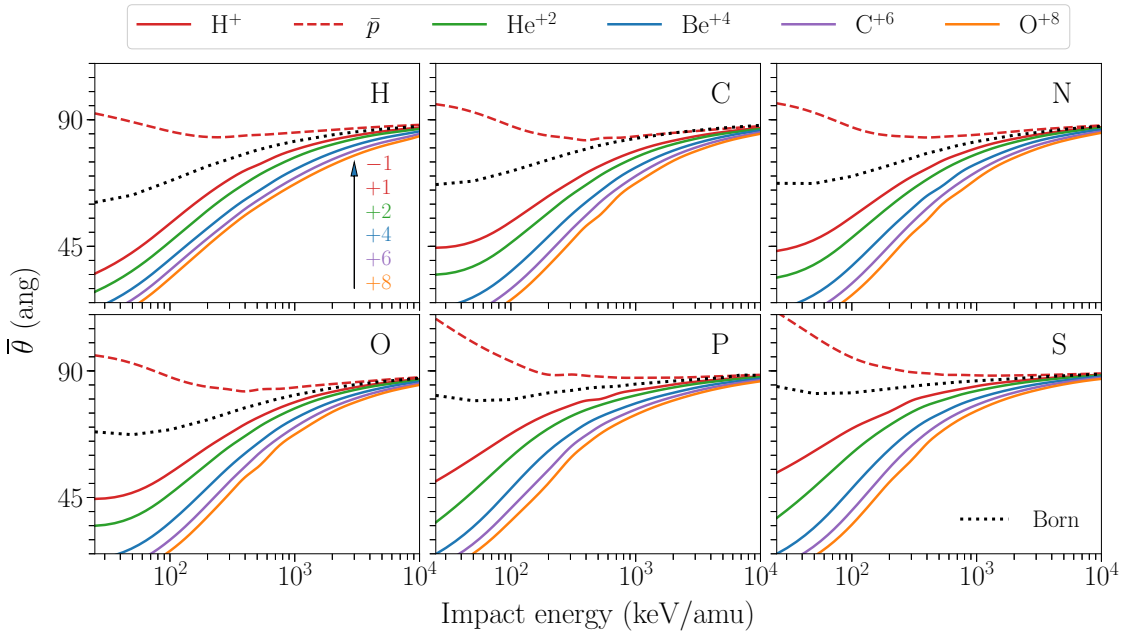

FIG. 3: Mean emitted angle distribution for ionization by impact of multicharged ions.

findings [27]. As can be noted in the figure, the mean energy value is surprisingly sensible to the projectile charge Z, which can duplicate the proton results in the intermediate region, i.e. 100–400 keV/amu. The effect observed can be attributed to the depletion caused by the multicharged ions to the yields of low energy electrons. This behavior cannot be found in the first Born approximation, where the Z^2 law cancels the Z dependence in Eq. (2). At high energies, $\overline{E}_\alpha$ tends to a universal value for all ions, as can be seen in Fig. 2.

B. Emitted electron angles

As mentioned before, secondary electrons contribute to the total damage. Then, not only is the ejection energy important but also the angle of emission. Once again, we can consider the single differential cross section in terms of the ejected electron solid angle Ω, $d\sigma_{\alpha,nl}/d\Omega$, to be expressed as a distribution function, and the mean angle $\overline{\theta}_\alpha$ can be defined as

$$\overline{\theta}_\alpha = \frac{\langle\theta_\alpha\rangle}{\langle 1\rangle} = \frac{1}{\sigma_\alpha}\sum_{nl}\int d\Omega\,\theta\,\frac{d\sigma_{\alpha,nl}}{d\Omega} \tag{4}$$

The mean emitted electron angles $\overline{\theta}_\alpha$ for the six atoms of interest are shown in Fig. 3, and an important dependence of $\overline{\theta}_\alpha$ with Z is observed. Once again, this effect is not observed in the first Born approximation. It is a general belief [34] that the angular dispersion of emitted

electrons are nearly isotropic. This behavior is caused by the insignificant angular anisotropy of sub–50–eV yield. A typical value for the ejection angle considered in the literature is $\overline{\theta}_\alpha \sim 70^\circ$ [27], and it is quite correct in the range of validity of the first Born approximation for any target. But, when a distorted wave approximation is used, $\overline{\theta}_\alpha$ decreases substantially with Z in the intermediate energy region, as observed in Fig. 3. For example, for C^{+6} impact, the Bragg peak occurs at 0.3 MeV/amu, where $\overline{\theta}_\alpha$, computed with the CDW method, is about half of the value obtained with the first Born approximation. This correction closes the damage to the forward direction.

We can attribute this forward direction correction to the capture to the continuum effect; the larger the charge Z, the smaller $\overline{\theta}$ will be. Of course, this effect only holds at intermediate energies and not at high impact energies, where the Born approximation rules. One illustrative observation is the behavior of antiprotons: the projectile in this case repels the electrons, being $\overline{\theta}_\alpha \sim 90^\circ$. Note the opposite effect of proton and antiprotons; they run one opposite to the other, as compared with the first Born approximation, constituting an angular Barkas effect.

III. IONIZATION OF MOLECULES

A. The stoichiometric model

Lets us consider a molecule M composed by n_α atoms of the element α, the SSM approaches the total ionization cross section of the molecule σ_M as a sum of ionization cross sections of the isolated atoms σ_α weighted by n_α,

$$\sigma_M = \sum_\alpha n_\alpha \sigma_\alpha \,. \tag{5}$$

We classified the molecular targets of our interest in three families: CH, CHN and DNA, as in Table I.

CH	CH_4 (methane), C_2H_2 (acetylene), C_2H_4 (ethene), C_2H_6 (ethane), C_6H_6 (benzene)
CHN	C_5H_5N (pyridine), $C_4H_4N_2$ (pyrimidine), C_2H_7N (dimenthylamine), CH_5N (monomethylamine)
DNA	$C_5H_5N_5$ (adenine), $C_4H_5N_3O$ (cytosine), $C_5H_5N_5O$ (guanine), $C_5H_6N_2O_2$ (thymine), $C_4H_4N_2O_2$ (uracil), C_4H_8O (THF), $C_5H_{10}O_5P$ (DNA backbone), $C_{20}H_{27}N_7O_{13}P_2$ (dry DNA)

TABLE I: Molecular targets studied in this work, classified in three families.

In Fig. 4, we report the total ionization cross sections by the impact of multicharged ions for adenine, cytosine, guanine and thymine. For adenine, the agreement with the experimental data available [9] is very good. To the best of our knowledge, there are not experimental data on ion–collision ionization for the rest of the molecules. We included electron impact measurements [10] with the corresponding equivelocity conversion for incident energies higher than 300 eV. In this region, the proton and electron cross section should converge. Although the electron impact measurements are above our findings for all the molecular targets, it is worth stating that our results agree very well with other electron impact theoretical predictions [11, 12].

Our results for uracil, DNA backbone, pyrimidine and THF are displayed in Fig. 5. For uracil, the agreement with the experimental proton impact measurements by Itoh *et al.* [13] is good. However, for the same target, our theory fails by a factor of two for the experimental ionization values by the impact of C^{+4}, O^{+6} and O^{+8} ions [14, 15]. Nonetheless, it should be stated that our theoretical results coincide with calculations by Champion, Rivarola and collaborators [14, 16], which may indicate a possible misstep of the experiments. For pyrimidine, we show comparison of our results with experimental data for proton [17] and electron [18] ionization. The electron impact measurements agree with our calculations for energies higher than 500keV. Unexpectedly, the proton impact cross sections are significantly lower than our findings. The THF molecule results are compared with proton [19] and electron [18, 20, 21] impact measurements, showing overall good agreement with our theory.

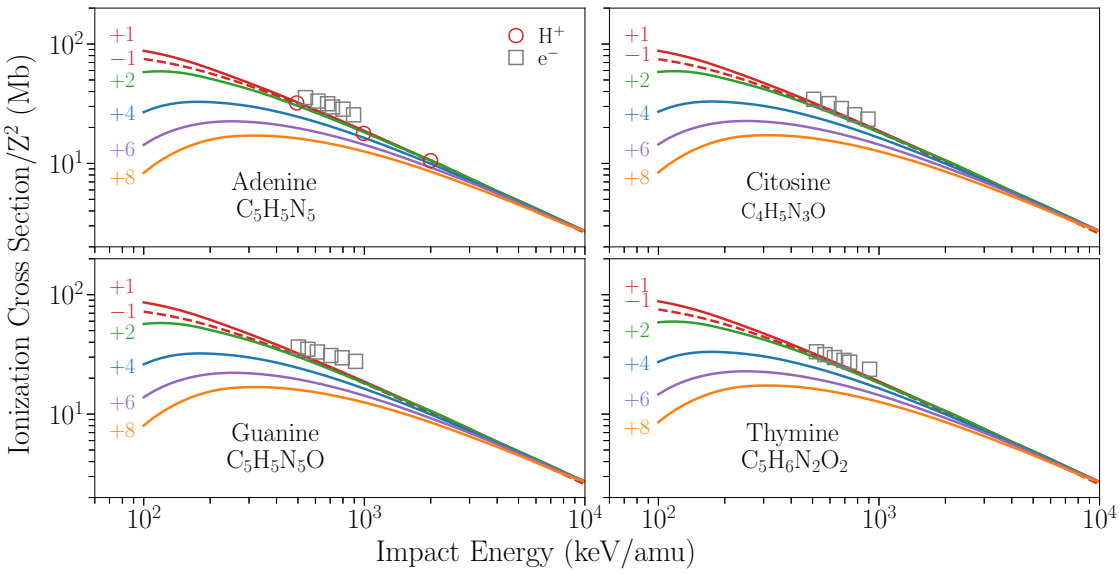

FIG. 4: Reduced CDW ionization cross section by impact of multicharged ions. Experiments: ○ [9] for proton impact and □ [10] for electron impact with equivelocity conversion.

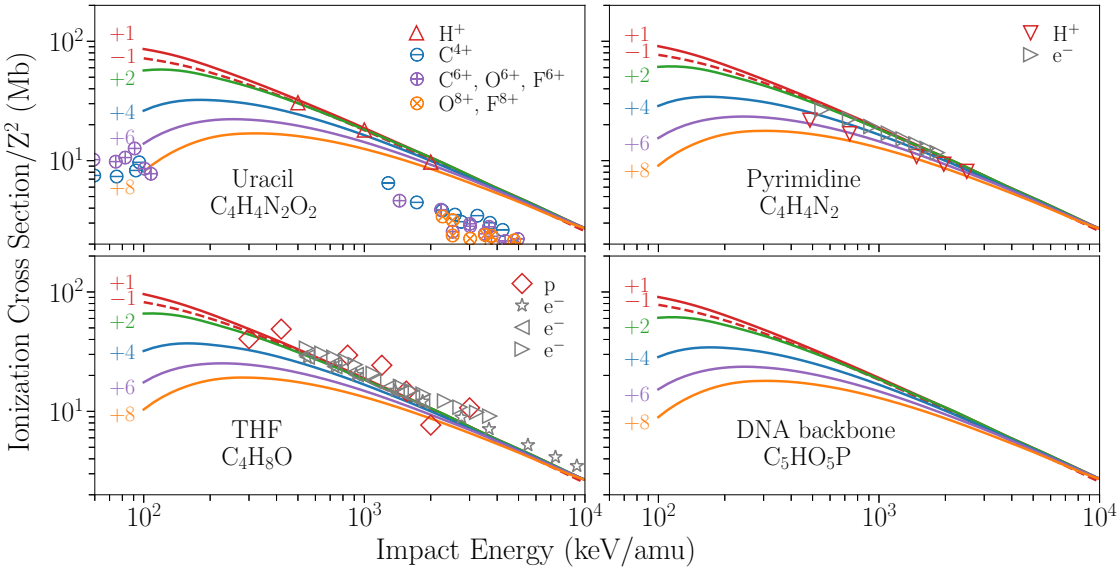

FIG. 5: Reduced CDW ionization cross section by impact of multicharged ions. Experiments: proton impact on △ uracil [13], ▽ pyrimidine [17] and ◇ THF [19]. Impact of ⊖ C^{+4}, ⊟ C^{+6}, O^{+6}, F^{+6}, and ⧋ O^{+8}, F^{+8} on uracil [14, 15]. Symbols ▷ [18], ◁ [20], and ☆ [21] for electron impact with equivelocity conversion.

B. Scaling rule

1. *Toburen rule*

The first attempt to develop a comprehensive but straightforward phenomenological model for electron ejection from large molecules was proposed by Toburen and coworkers [25, 26]. The authors found it convenient to scale the experimental ionization cross section in terms of the number of weakly–bound electrons, n_e. For instance, for C, N, O, P and S, this number is the total number of electrons minus the K–shell. Following Toburen, the scaled ionization cross section per weakly bound electron σ_e^T is

$$\sigma_e^T = \frac{\sigma_M}{n_e}\,, \tag{6}$$

where $n_e = \sum_\alpha n_\alpha \nu_\alpha^T$, and ν_α^T are the Toburen numbers given by

$$\nu_\alpha^T = \begin{cases} 1, \text{ for H,} \\ 4, \text{ for C,} \\ 5, \text{ for N and P,} \\ 6, \text{ for O and S}\,. \end{cases} \tag{7}$$

The Toburen rule can be stated by saying that σ_e is a *universal* parameter independent on the molecule, which depends solely on the impact velocity, and holds for high impact energies (i.e. 0.25–5 MeV/amu). These ν_α^T can be interpreted as the number of active electrons in the collision. Of course, at very high energies also de K–shell electrons will be ionized and these numbers will be different. A similar dependence with the number of weakly bound electrons was found in Ref. [13] for proton impact on uracil and adenine.

By implementing the SSM, we computed the scaled CDW cross sections σ_e^T for the molecular targets of Table I. Our results are shown in Fig. 6a as a function of the impact energy for different projectile charges. Although the Toburen scaling holds for high energies, its performance is still not satisfactory: the universal band is quite broad, as can be noted in Fig. 6a.

2. *New scaling*

The departure of our theoretical results from the Toburen rule can be easily understood by inspecting Fig. 1. It can be noted that the rule $\sigma_\alpha/\nu_\alpha^T \sim \sigma_e^T$, approximatelly constant, is

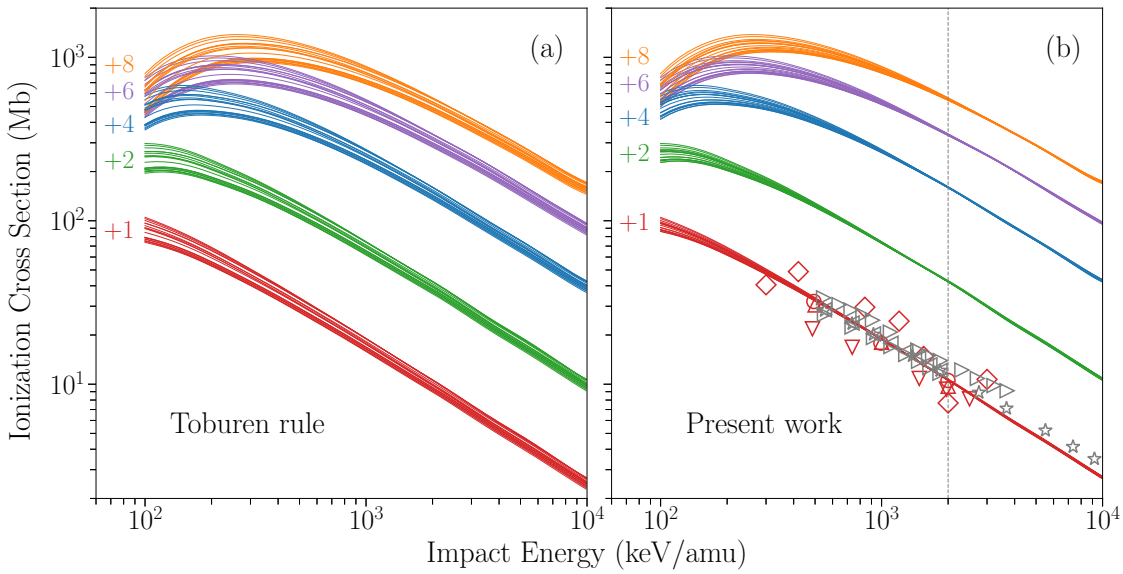

FIG. 6: Scaled ionization cross section per weakly bound electron using (a) the Toburen numbers ν_α^T, and (b) our proposed numbers $\nu_\alpha^{\rm CDW}$. Experiments: proton impact on ○ adenine [9], △ uracil [13], ▽ pyrimidine [17] and ◇ THF [19]; electron impact on ▷ pyrimidine [18], and ◁, ☆ [20, 21] THF.

not well satisfied by the CDW. For example, Fig. 1 shows that the cross sections for O are actually very similar to the cross sections for C, suggesting 4 active electrons in O instead of 6. In the same way, the number of active electrons for N, P and S are also different from the ν_α^T of Eq. (7).

Based on the CDW results, we propose a new scaling,

$$\sigma_e = \frac{\sigma_M}{n_e'}, \tag{8}$$

where $n_e' = \sum_\alpha n_\alpha \nu_\alpha^{\rm CDW}$, and $\nu_\alpha^{\rm CDW}$ are the numbers of active electrons per atom obtained from the CDW ionization cross sections for different ions in H, C, N, O, P , and S targets, given as follows,

$$\nu_\alpha^{\rm CDW} \sim \begin{cases} 1, & \text{for H,} \\ 4, & \text{for C, N, and O,} \\ 4.5, & \text{for P and S.} \end{cases} \tag{9}$$

The new scaled cross sections σ_e are plotted in Fig. 6b. A much better sharp band is observed, especially for impact energies $E = (0.5 - 8)$ MeV/amu for $Z = 1$ and $Z = 2$, and $E = (2.5 - 8)$ MeV/amu for $Z > 2$. In fact, the experimental data for ionization of

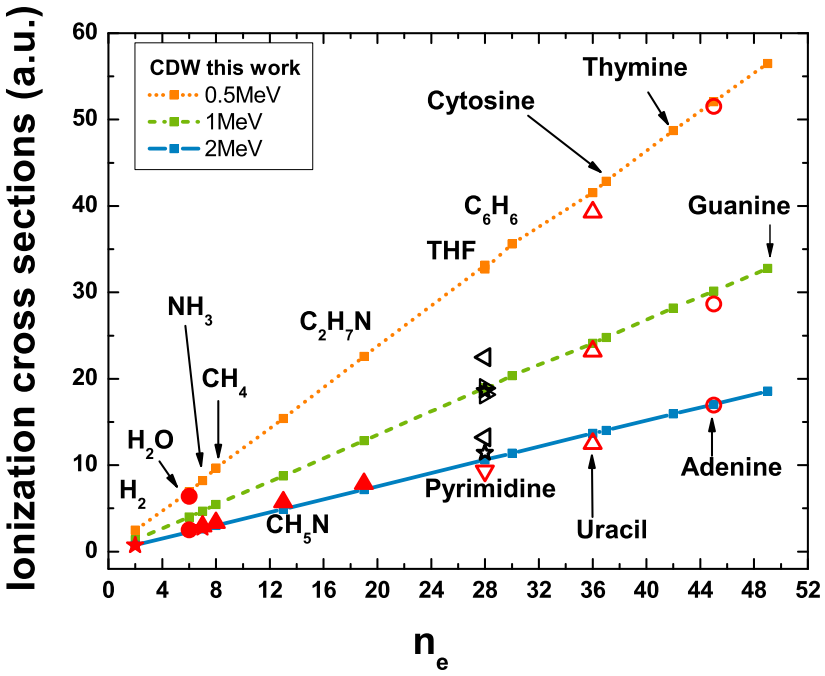

FIG. 7: Ionization cross sections by impact of protons at 0.5, 1 and 2 MeV in terms of the number of active electrons given by Table II. Experiments: ○ adenine [9], △ uracil [13], ▽ pyrimidine [17], ▲ $C2H_7N$, CH_5N, methane and amonia [22], ★ amonia and H_2 [23], and ● water [24].

adenine [9], uracil [13], pyrimidine [17] and THF [19] by proton impact in Fig. 6b seems to corroborate the new scaling. We also included the electron impact ionization measurements with equivelocity conversion on pyrimidine [18], and THF [18, 20, 21]. It will be interesting to cross–check for experiments with higher projectile charge states.

Molecule	n_e	Molecule	n_e	Molecule	n_e
H_2	2	C_2H_7N	19	$C_4H_5N_3O$	37
H_2O	6	C_4H_8O	28	$C_5H_6N_2O_2$	42
NH_3	7	$C_4H_4N_2$	28	$C_5H_5N_5$	45
CH_4	8	C_6H_6	30	$C_5H_5N_5O$	49
CH_5N	13	$C_4H_4N_2O_2$	36	$C_5H_{10}O_5P$	54.5

TABLE II: New scaling numbers for some molecular targets of biological interest.

By using Eq. (9), we define new active electron numbers n'_e for some molecular of interest

in Table II. These values are very different from the ones proposed by Toburen and used by other authors [13]. Moreover, an alternative way of showing the scaling can be attained by plotting the ionization cross sections of molecules as a function of the number of active electrons from Table II. Our findings are displayed in Fig. 7 for impact energies 0.5, 1 and 2 MeV. As can be noted, the computed CDW ionization cross sections for all the molecules show a linear dependence with the number of electrons from Table II. We obtain similar results even for E = 10 MeV. The comparison with the experimental data available shows very nice agreement, from the smallest molecules, H_2, H_2O and CH_4, up to the most complex ones, like adenine. For electron impact data, the experimental data was interpolated between close neighboors.

C. Molecular structure of targets

To test the range of validity of the SSM, we performed a full molecular structure calculation of five nucleobases. We employed the GAMESS code and used the 6-31G(d,p) basis set, which includes polarization functions for all the atoms. The calculations were carried out implementing the B3LYP functional [31, 32] to account for the correlation and exchange effects.

The molecular binding energies of the valence electrons for adenine, cytosine, guanine, thymine and uracil are shown in Fig. 8. We can compute the center of gravity of the molecular energy levels as an average weighted by the electronic occupation number. The results obtained from the full molecular calculation are given in the first row of Table III. Similarly, we can compute the baricenter of the energy levels defined by the Toburen rule and the one given by Eq. (9), which are also given in Table III. The average energy values obtained from the Toburen rule are around 20% of the full molecular ones. Surprisingly, the new scaling rule gives a significant improvement in the average energy values, reducing the relative errors to about 7%. This improvement would seem to indicate that the new scaling is appropiate.

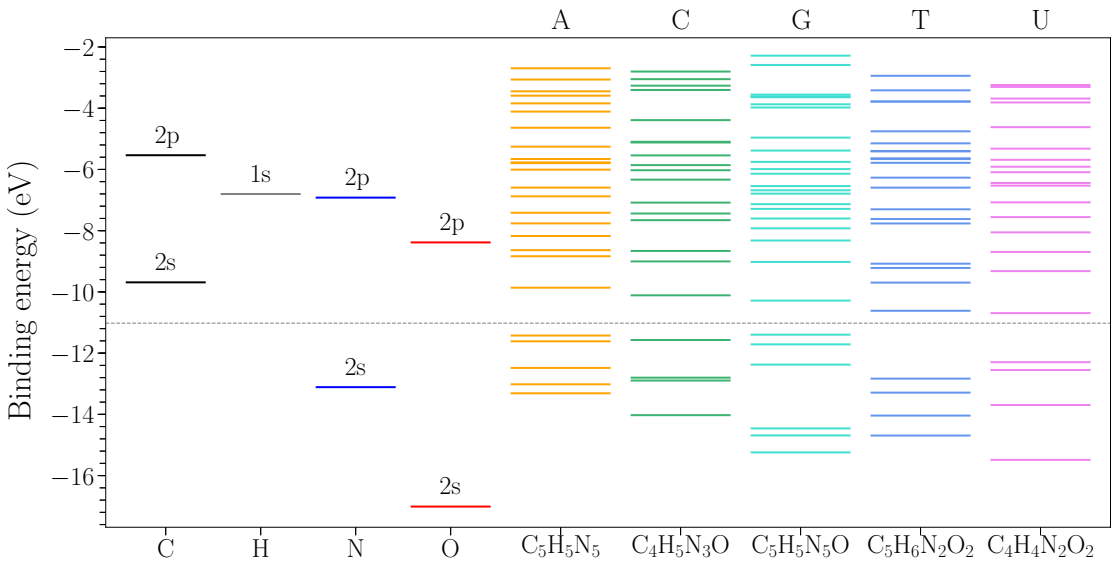

FIG. 8: Theoretical molecular binding energies for adenine, cytosine, guanine, thymine and uracil compared to those of atomic constituents.

E_{av} (eV)	A	C	G	T	U
	$C_5H_5N_5$	$C_4H_5N_3O$	$C_5H_5N_5O$	$C_5H_6N_2O_2$	$C_4H_4N_2O_2$
Theoretical calc.	−7.1955	−6.9058	−7.4725	−7.5304	−7.6224
Toburen rule	−8.4236	−8.6743	−8.7275	−8.7947	−9.0022
Present work	−7.9027	−7.8639	−7.9420	−7.8066	−7.8839

TABLE III: Center of gravity of the molecular energy levels of five nucleobases.

Furthermore, on the left side of the Fig. 8, we show the atomic Hartree–Fock energies of the constituent elements, which gives an insight on the distribution of the weakly bound electrons. A dashed line around −11 eV is drawn to separate the band in two. We can consider the atomic energy levels above this line as the ones corresponding to the weakly bound electrons from Eq. (9). For example, the $2s$ and $2p$ electrons of carbon are placed above the separating line, which corresponds to the 4 electrons given by Eq. (9). In the case of O, only the 4 electrons of the $2p$ orbitals are located above the separating line.

The electrons in the molecular targets corresponding to the $2s$ of N and C in the atomic case are placed in a secondary gap. The lower levels of the secondary gap correspond to the oxygen. The number of electrons in the valence shell for all O would seem to be equal to

4, as previously setted by the scaling rule Eq. (9). The N case is not as straightfoward; the electrons that would correspond to the $2s$ are located just below the line. The $\nu_\alpha^{\mathrm{CDW}}$ value given for N would suggest that a significant amount of electron density from the secondary gap is shared with the valence band.

The SSM considers the molecule to be assembled by isolated neutral atoms, which is definitively unrealistic. A first improvement can be suggested by assuming that the atoms are not neutral and that they have an uneven distribution of electrons within the molecule; this distribution can be given by an effective charge q_α. A possible value for q_α is given by the Mulliken charge. However, there are a wide variety of charge distributions, such as the net or natural atomic charge [29], the Löwdin charge, etc.

Consider that the total amount of electrons Q_α on the element α are equally distributed on all the α atoms. Therefore, each element α will have an additional charge: $q_\alpha = Q_\alpha/n_\alpha$, which can be positive or negative. This value will depend on the relative electronegativity value with respect to the other atoms [30]. Now, instead of an integer number of elements n_α of the atom α, we have a fractional number of atoms given by

$$n'_\alpha = n_\alpha - \frac{q_\alpha}{\nu_\alpha^{\mathrm{CDW}}} \tag{10}$$

In the case of neutral atoms, $q_\alpha = 0$ and we recover $n'_\alpha = n_\alpha$, as it should be.

In Table IV, we display the charge q_α of four DNA molecules, obtained from the full molecular calculation.

Element	C	H	N	O	New stoichiometry
Adenine	+0.32	+0.23	–0.55		$C_{4.92}H_{4.77}N_{5.14}$
Cytosine	+0.28	+0.21	–0.56	–0.53	$C_{3.93}H_{2.79}N_{5.14}O_{1.13}$
Guanine	+0.46	+0.20	–0.58	–0.36	$C_{4.89}H_{4.80}N_{5.15}O_{1.09}$
Thymine	+0.20	+0.19	–0.54	–0.52	$C_{4.95}H_{1.95}N_{6.13}O_{2.13}$

TABLE IV: Effective charge q_α and new stoichiometric formula defined by Eq. (10) for four DNA molecules.

By implementing Eq. (10), it is possible to determine a new stoichiometric formula (last column of Table IV). Now, instead of having an integer number of atoms n_α, we obtain a fractional number n'_α. Molecular cross sections σ' can be computed considering such values.

Relative errors for the ionization cross sections were computed for the DNA bases from Table IV. The differences obtained were of just very few percents, which indicates that the modified SSM is a quite robust model to handle these type of molecule within the range error expected for this model.

IV. CONCLUSIONS

We calculated ionization cross sections by impact of antiprotons, H^+, He^{+2}, Be^{+4}, C^{+6}, and O^{+8} for seventeen molecules containing H, C, N, O, P and S with the CDW method. The importance of the influence of Z was observed in the mean energy $\overline{E}_\alpha$ and angle $\overline{\theta}_\alpha$. For a given target α, as the nuclear charge of the projectile Z increases, so does the mean energy of emittion $\overline{E}_\alpha$. Conversely, the mean angle of emission $\overline{\theta}_\alpha$ decreases. At high impact energy, say larger than 1 MeV/amu, these values converge to the Born approximation, which embodies the simple Z^2 law. The seventeen molecules selected were investigated using the simple stoichiometric model. Results for eigth DNA bases were presented and compared with the sparse available experiments. We explore the rule of Toburen which scales all the molecular ionization cross section when divided by the number of weakly bound valence electrons ν_α^T given by Eq. (6). We found the rule scales much better when normalizing our theoretical ionization cross sections to the number $\nu_\alpha^{\rm CDW}$ given by Eq. (9). Finally, we attempt to improve the stoichiometric model by using the Mulliken charge to define a new model containing fractional rather than integer proportions. No substantial correction was found, which indicates that our modified SSM works quite well. By inspecting the molecular binding energy from quantum mechanical structure calculations, we were able to understand the values defined for $\nu_\alpha^{\rm CDW}$.

The main objective of this article is to provide the tools to estimate any inelastic parameter parameter –such as emission angle, emitted mean energy and cross section– by the impact of any multicharged on any molecule containing H, C, N, O, P and S, with the help of the stoichimetrical model. Our goal was quite ambitious, considering the simplicity of our proposal. However, we think our results could be used to estimate the ionization magnitude with an acceptable level of uncertainty.

[1] M. W. Schmidt, K. K. Baldridge, J. A. Boatz, S. T. Elbert, M. S. Gordon, J. H. Jensen, S. Koseki, N. Matsunaga, K. A. Nguyen, S. J. Su, T. L. Windus, M. Dupuis, J. A. Montgomery J. Comput. Chem. 14, 1347-1363 (1993)

[2] J. E. Miraglia and M. S. Gravielle. Ionization of the He, Ne, Ar, Kr, and Xe isoelectronic series by proton impact. Phys Rev A **78**, 052705 (2008)

[3] J. E. Miraglia, Ionization of He, Ne, Ar, Kr, and Xe by proton impact: Single differential distributions. Phys. Rev. A **79**, 022708 (2009).

[4] Salvat, F., Fernndez-Varea, J.M., Williamson, W. Comput. Phys. Commun. **90**, 151–168 (1995)

[5] A.M.P. Mendez, D.M. Mitnik, and J.E. Miraglia. Depurated inversion method for orbital-specific exchange potentials. Int. J. Quantum Chem. 24 ,116 (2016).

[6] A.M.P. Mendez, D.M. Mitnik, and J.E. Miraglia. Local Effective Hartree–Fock Potentials Obtained by the Depurated Inversion Method, 76. (2018).

[7] Ionization probabilities of Ne, Ar, Kr, and Xe by proton impact for different initial states and impact energies. Nucl. Instr. Meth. Phys. Res. B 407 (2017) 236-243.

[8] J. E. Miraglia. Shell-to-shell ionization cross sections of antiprotons, H^{+}, He^{+2}, Be^{+4}, C^{+6} and O^{+8} on H, C, N, O, P, and S atoms To be published Archive 2019.

[9] Y. Iriki, Y. Kikuchi, M. Imai, and A. Itoh Phys. Rev. A **84** 052719 (2011).

[10] M. A. Rahman and E. Krishnakumar, Electron ionization of DNA bases, J. Chem. Phys. **144**, 161102 (2016).

[11] P. Mozejko and L. Sanche, Cross section calculations for electron scattering from DNA and RNA bases. Radiat Environ. Biophys **42**, 201 (2003).

[12] H. Q. Tan, Z. Mi, and A. A. Bettiol, Simple and universal model for electron-impact ionization of complex biomolecules, Phys. Rev. E 97, 032403 (2018)

[13] A. Itoh, Y. Iriki, M. Imai, C. Champion, and R. D. Rivarola, Cross sections for ionization of uracil by MeV-energy-proton impact, Phys. Rev. A **88**, 052711 (2013).

[14] A. N. Agnihotri, S. Kasthurirangan, S. Nandi, A. Kumar, M. E. Galassi, R. D. Rivarola, O. Fojón, C. Champion, J. Hanssen, H. Lekadir, P. F. Weck, and L. C. Tribedi. Ionization of uracil in collisions with highly charged carbon and oxygen ions of energy 100 keV to 78 MeV.

Phys. Rev. A 85, 032711 (2012).

[15] A N Agnihotri, S Kasthurirangan, S Nandi, A Kumar, C Champion,, H Lekadir, J Hanssen, P FWeck, M E Galassi, R D Rivarola, O Fojon and L C Tribedi, Absolute total ionization cross sections of uracil ($C_4H_4N_2O_2$) in collisions with MeV energy highly charged carbon, oxygen and fluorine ions J. Phys. B **46**, 185201 (2013).

[16] C Champion, M E Galassi, O Fojón, H Lekadir, J Hanssen, R D Rivarola, P F Weck, A N Agnihotri, S Nandi, and L C Tribedi. Ionization of RNA-uracil by highly charged carbon ions. J. Phys.: Conf. Ser. **373**, 012004 (2012).

[17] W. Wolff, H. Luna, L. Sigaud, A. C. Tavares, and E. C. Montenegro Absolute total and partial dissociative cross sections of pyrimidine at electron and proton intermediate impact velocities J. Chem. Phys. **140**, 064309 (2014).

[18] M. U. Bug, W. Y. Baek, H. Rabus, C. Villagrasa, S. Meylan, A. B. Rosenfeld, An electron-impact cross section data set (10 eV–1 keV) of DNA constituents based on consistent experimental data: A requisite for Monte Carlo simulations, Rad. Phys. Chem. **130** 459–479 (2017).

[19] M. Wang, B. Rudek, D. Bennett, P. de Vera, M. Bug, T. Buhr, W. Y. Baek, G. Hilgers, H. Rabus, Cross sections for ionization of tetrahydrofuran by protons at energies between 300 and 3000 keV Phys. Rev. A **93**, 052711 (2016).

[20] W. Wolff, B. Rudek, L. A. da Silva, G. Hilgers, E. C. Montenegro, M. G. P. Homem, Absolute ionization and dissociation cross sections of tetrahydrofuran: Fragmentation–ion production mechanisms J. Chem. Phys. **151**, 064304 (2019).

[21] M. Fuss, A. Muoz, J. C. Oller, F. Blanco, D. Almeida, P. Limo-Vieira, T. P. D. Do, M. J. Brunger, G. Garca, Electron-scattering cross sections for collisions with tetrahydrofuran from 50 to 5000 eV Phys. Rev. A **80**, 052709 (2009).

[22] D. J. Lynch, L. H. Toburen, and W. E. Wilson, Electron emission from methane, ammonia, monomethylamine, and dimethylamine by 0.25 to 2.0 MeV protons J. Chem. Phys. **64**, 2616 (1976).

[23] M.E. Rudd, Y.-K. Kim, D.H. Madison, J.W. Gallagher, Electron production in proton collisions: total cross sections, Review of Modern Physics, **57**, 965–994 (1985).

[24] H. Luna, A. L. F. de Barros, J. A. Wyer, S. W. J. Scully, J. Lecointre, P. M. Y. Garcia, G. M. Sigaud, A. C. F. Santos, V. Senthil, M. B. Shah, C. J. Latimer, and E. C. Montenegro,

Water-molecule dissociation by proton and hydrogen impact, Phys. Rev. A **75** 042711 (2007).

[25] W. E. Wilson and L. H. Toburen. Electron emission from proton –hydrocarbon-molecule collisions at 0.3–2.0 MeV. Phys. Rev. A 11, 1303 (1975).

[26] D. J. Lynch, L. H. Toburen, and W. E. Wilson. Electron emission from methane, ammonia, monomethylamine, and dimethylamine by 0.25 to 2.0 MeV protons. J. Chem. Phys. 64, 2616 (1976).

[27] Multiscale approach to the physics of radiation damage with ions. E. Surdutovich and A. V. Solov'yov, arXiv:1312.0897v, (2013)

[28] P. de Vera1, I. Abril, R. Garcia-Molina and A.V.Solov'yov, Ionization of biomolecular targets by ion impact: input data for radiobiological applications. Journal of Physics: Conference Series 438 (2013) 012015

[29] Jung-Goo Lee, Ho Young Jeong, and Hosull Lee, Charges of Large Molecules Using Reassociation of Fragments. Bull. Korean Chem. Soc.24 2003, 369 .

[30] A. K. Rappe, A. K.and W. A. Goddard III,. J. Phys. Chem. **95 (**1991) 3358.

[31] A. D. Becke, J. Chem. Phys. 98, 5648-5652 (1993)

[32] P. J. Stephens, F. J. Devlin, C. F. Chabalowski, M. J. Frisch, J. Phys. Chem. 98, 11623-11627 (1994)

[33] S.M. Pimblott and J. A. LaVerne, Radiation Physics and Chemistry 76, 1244-1247 (2007)

[34] M. E. Rudd, Y.-K. Kim,, D. H. Madison and T. J. Gay. Electron production in proton collisions with atoms and molecules: energy distributions. Rev. Mod. Phys. **64**, 44-490 (1992).

[35] E. Clementi, C. Roetti, At. Data Nucl. Data Tables 14, 177–478 (1974).